Determination of the Chemical Nature of Active Surface Sites Present on Bulk Mixed Metal Oxide Catalysts†

Israel E. Wachs,*,‡ Jih-Mirn Jehng,§ and Wataru Ueda||

Operando Molecular Spectroscopy and Catalysis Laboratory, Department of Chemical Engineering, Lehigh University, Bethlehem, Pennsylvania 18015, Department of Chemical Engineering, National Chung Hsing University, Taichung 402, Republic of China, and Catalysis Research Center, Hokkaido University, N-11, S-10, Kita-ku, Sapporo 060-0811, Japan

Received: March 15, 2004; In Final Form: June 17, 2004

CH_3OH temperature programmed surface reaction (TPSR) spectroscopy was employed to determine the chemical nature of active surface sites for bulk mixed metal oxide catalysts. The CH_3OH-TPSR spectra peak temperature, T_p, for model supported metal oxides and bulk, pure metal oxides was found to be sensitive to the specific surface metal oxide as well as its oxidation state. The catalytic activity of the surface metal oxide sites was found to decrease upon reduction of these sites and the most active surface sites were the fully oxidized surface cations. The surface V^{5+} sites were found to be more active than the surface Mo^{6+} sites, which in turn were significantly more active than the surface Nb^{5+} and Te^{4+} sites. Furthermore, the reaction products formed also reflected the chemical nature of surface active sites. Surface redox sites are able to liberate oxygen and yield H_2CO, while surface acidic sites are not able to liberate oxygen, contain either H^+ or oxygen vacancies, and produce CH_3OCH_3. Surface V^{5+}, Mo^{6+}, and Te^{4+} sites behave as redox sites, and surface Nb^{5+} sites are Lewis acid sites. This experimental information was used to determine the chemical nature of the different surface cations in bulk Mo−V−Te−Nb−O_x mixed oxide catalysts ($Mo_{0.6}V_{1.5}O_x$, $Mo_{1.0}V_{0.5}Te_{0.16}O_x$, $Mo_{1.0}V_{0.3}Te_{0.16}Nb_{0.12}O_x$). The bulk $Mo_{0.6}V_{1.5}O_x$ and $Mo_{1.0}V_{0.5}Te_{0.16}O_x$ mixed oxide catalytic characteristics were dominated by the catalytic properties of the surface V^{5+} redox sites. The surface enrichment of these bulk mixed oxide by surface V^{5+} is related to its high mobility, V^{5+} possesses the lowest Tammann temperature among the different oxide cations, and the lower surface free energy associated with the surface termination of V═O bonds. The quaternary bulk $Mo_{1.0}V_{0.3}Te_{0.16}Nb_{0.12}O_x$ mixed oxide possessed both surface redox and acidic sites. The surface redox sites reflect the characteristics of surface V^{5+} and the surface acidic sites reflect the properties normally associated with supported Mo^{6+}. The major roles of Nb^{5+} and Te^{4+} appear to be that of ligand promoters for the more active surface V and Mo sites. These reactivity trends for CH_3OH ODH parallel the reactivity trends of propane ODH because of their similar rate-determining step involving cleavage of a C−H bond. This novel CH_3OH-TPSR spectroscopic method is a universal method that has also been successfully applied to other bulk mixed metal oxide systems to determine the chemical nature of the active surface sites.

Introduction

The foundation for a revolution in metal catalysis science took place during the 1960s and 1970s when CO, H_2, O_2, and N_2O selective chemisorption methods were developed to quantitatively determine the number of exposed metal atoms in metal catalysts.[1] The seed for this development was the pioneering studies by Emmett and Brunauer when they employed selective CO chemisorption to determine the number of exposed metallic iron atoms and CO_2 chemisorption to determine the number of exposed basic potassium oxide promoter atoms on the surface of ammonia synthesis catalysts.[2] Knowledge of the number of surface metal atoms allowed, for the first time, the systematic use of turnover frequency (TOF, the number of molecules reacted per surface metal atom per second) for comparison of catalytic reactions between different investigators as well as between large metallic single crystals and supported metal powders with large specific surface areas. This led to the concept of structure-sensitive and structure-insensitive catalytic reactions.[1] Structure-insensitive reactions exhibit the same TOF values for all metal crystal sizes and are independent of specific crystallographic orientations. Structure-sensitive reactions, however, exhibit TOF values that are dependent on the metal crystal size and the specific crystallographic orientation. Furthermore, it was found that structure-insensitive catalytic reactions are not strongly affected by the nature of the metal, alloying, and poisoning and can be described by uniform surface kinetics. In contrast, structure-sensitive catalytic reactions are very strongly affected by the specific metal, alloying, and poisoning and cannot be described by uniform surface kinetics. Only kinetics based on nonuniform surface Temkin formalism is able to satisfactorily describe structure-sensitive catalytic reactions (e.g., ammonia synthesis from N_2 and H_2 over metallic Fe catalysts).

Djega-Mariadassou et al. stated in the early 1980s that the progress made in the case of metal catalysts should also follow for metal oxides,[3] in particular, comparisons between the

† Part of the special issue "Michel Boudart Festschrift".
‡ Lehigh University.
§ National Chung Hsing University.
|| Hokkaido University.

10.1021/jp048839e CCC: $30.25
Published on Web 08/28/2004

catalytic activity of large single crystals and powders with large specific surface areas. This development, however, has been slow in coming over the past two decades because satisfactory selective chemisorption techniques for metal oxides have not been developed and adopted by the catalysis researcher community. Djega-Mariadassou et al.[3] and Sleight et al.[4] independently demonstrated in the 1980s that alcohols are feasible for selective chemisorption studies of metal oxides with surfaces of preferred orientation. However, these initial selective chemisorption studies on ZnO,[3] MoO_3, [4] and $Fe_2(MoO_4)_3$ [4] powders were not successfully extended to other metal oxide catalytic systems until very recently.[5−8] A major hurdle in comparing large single crystal metal oxides and metal oxide powders with high surface areas is that the surfaces of the large single crystals are typically prepared in ultrahigh vacuum (UHV) and, consequently, do not form the same surface structures and functionalities as metal oxide powders. For example, metal oxide surfaces prepared in a vacuum do not terminate in M−OH functionalities and many times cannot easily be fully oxidized at lower O_2 pressures typically employed.[10,11] Metal oxides are also much more complex catalytic materials than metals because of their variable oxidation states, variable coordination for each oxidation state, distribution of surface redox, basic and acidic sites, distribution among surface Lewis and Bronsted acidic sites, and participation of surface and bulk lattice oxygen atoms in catalytic oxidation reactions. Thus, this multidimensional issue for metal oxides requires not only selective chemisorption methods that provide information about the number of active surface sites but also information that is very rich in the chemical nature of the active sites. The present study demonstrates how this has been achieved for bulk Mo−V−Nb−Te−O mixed metal oxides by employing CH_3OH temperature programmed surface reaction (TPSR) spectroscopy.

Experimental Section

Catalyst Preparation. The Nb_2O_5 (BET = 57 m^2/g) was synthesized by air calcination of niobium oxide hydrate ($Nb_2O_5 \cdot nH_2O$ from CBMM, 99.9% purity) at 500 °C for 10 h. The resulting Nb_2O_5 was also employed as an oxide support for vanadia, molybdena, telluria, and their combinations. The supported V_2O_5/Nb_2O_5 catalysts were prepared by incipient-wetness impregnation of the Nb_2O_5 support with 2-propanol solutions of vanadium isopropoxide (Alfa Aesar, 97% purity). The preparation was formed inside a glovebox with continuously flowing N_2. After impregnation, the samples were kept inside the glovebox with flowing N_2 overnight. The samples were further dried in flowing N_2 at 120 °C for 1 h and calcined in flowing air at 450 °C for 2 h. The supported MoO_3/Nb_2O_5 and TeO_2/Nb_2O_5 samples were prepared by the incipient-wetness impregnation of the Nb_2O_5 support with aqueous solutions of ammonium heptamolybdate (Matheson, Coleman & Bell, 99.9& purity) and telluric acid ($H_2TeO_4 \cdot 2H_2O$, Alfa Aesar), respectively. After impregnation, the samples were dried under ambient conditions for 48 h and calcined in air at 450 °C for 2 h. Combinations of these metal oxides on Nb_2O_5 were also prepared sequentially following the above syntheses procedures. The impregnation sequence procedure is reflected in the notation $BOx/AOx/Nb_2O_5$, where the A component was first impregnated onto the Nb_2O_5 support, dried, and calcined and then the BOx component was impregnated onto the calcined AOx/Nb_2O_5 catalyst, dried, and calcined. The notation of $BOx/AOx/Nb_2O_5$ was used to describe such double impregnated samples.

The bulk, pure metal oxides V_2O_5, MoO_3, and TeO_2 were prepared the same way as described above, but in the absence of the Nb_2O_5 support. The solutions were slowly precipitated by controlling the solution pH with ammonium hydroxide, dried, and finally calcined in air at 400 °C for 1 h. Raman characterization confirmed that the expected crystal phases were formed. The resultant BET surface areas were ∼3−5 m^2/g.

The bulk mixed metal oxides were prepared by hydrothermal synthesis. The starting materials were ammonium heptamolybdate, vanadyl sulfate, tellurium hydroxide, and niobium oxalate. These salts were used to make the initial aqueous solution slurry. The slurry was introduced into a stainless steel autoclave equipped with a Teflon inner tube. The hydrothermal reaction was carried out at 175 °C for different lengths of time for each combination of oxides: binary Mo−V−O for 20 h, tertiary Mo−V−Te−O for 48 h, and quaternary Mo−V−Te−Nb−O for 48 h. The resulting solids were separated by filtration, washed with distilled water, dried in air at 80 °C overnight, and calcined in a flowing N_2 stream at 600 °C for 2 h. The binary M−V−O mixed oxide was calcined at 500 °C in N_2 and the tertiary Mo−V−Te−O was precalcined in air at 280 °C prior to the high-temperature calcinations in N_2. The resulting bulk mixed metal oxide catalysts exhibited the orthorhombic X-ray diffraction (XRD) structure and comparable BET surface areas of 6−7 m^2/g.

Raman Spectroscopy. The in situ Raman spectrometer system consists of a quartz cell with a sample holder (Hastalloy C), a triple grating spectrometer (Spex, model 1877), a CCD detector (Jobin Yvon-Spex, ISA Inc., model Spectrum-1), and an argon ion laser (Spectra Physics, model 165). The sample typically contained 100−200 mg and was pressed into a disk shape so that it could be mounted in the sample holder. The sample holder was mounted onto a ceramic shaft that was rotated at 1000−2000 rpm by a 115 V dc motor. A cylindrical heating coil controlled the quartz cell temperature that was monitored by a thermocouple placed next to the catalyst sample inside the cell. The cell was capable of being heated to 600 °C, and gas flow rates of ∼100 cm^3/min at atmospheric pressure were typically employed.

CH_3OH-TPSR Spectroscopy. The CH_3OH-TPSR spectroscopy studies were performed with the AMI-100 temperature programmed system (Zeton-Altamira Instruments) equipped with an online mass spectrometer (Dycor DyMaxion, Ametek Process Instruments). Typically, about 25−100 mg of catalyst was loaded in a U-type quartz tube and pretreated at elevated temperatures to dehydrate the sample. The Nb_2O_5 and the niobia-supported metal oxides were pretreated in flowing dry air at 450 °C for 1 h. The bulk, pure oxides were pretreated in flowing dry air at 350 °C for 1 h. The bulk mixed metal oxides were treated in flowing He at 350 °C for 1 h to prevent their full oxidation. The supported and bulk, pure metal oxides were subsequently cooled in flowing O_2/He to ∼200 °C and then switched to a flowing He stream to flush out any residual gas-phase O_2. In the case of the bulk mixed metal oxide catalysts, the catalysts were cooled in a flowing He stream. For those experiments where the effect of CH_3OH-TPSR reduction was also examined, all the catalysts were cooled in flowing He so the reduced surface sites would not become oxidized upon cooling (referred to as CH_3OH-TPSR cycles in the paper). The metal oxide samples were all further cooled in He inert environments to the methanol adsorption temperature of ∼50 °C. Methanol adsorption was achieved by flowing 2000 ppm CH_3OH/He for 30 min, and the system was then purged with flowing He for another 30 min. Afterward, the catalysts were heated at a constant heating rate of 10 °C/min to 400−500 °C in flowing He (30 mL/min). The gases exiting from the quartz tube reactor

were analyzed with an online mass spectrometer, which was linked via a capillary tube, as a function of catalyst temperature. The following *m*/*e* ratios were employed for the identification of the various gases: CH_3OH, $m/e = 31$; H_2CO, $m/e = 30$; CH_3OCH_3, $m/e = 45$ and 15; H_2O, $m/e = 18$; H_3COOCH, $m/e = 60$; $(CH_3O)_2CH_2$, $m/e = 75$. The formation of CO_2/CO is not reported in the current studies because these reaction products primarily originate from reasdsorption of formaldehyde (via formation of surface formate species) or adsorption of background carbonaceous molecules during the CHOH-TPSR studies. Furthermore, formation of CO_2/CO was essentially not observed at low conversions during methanol oxidation steady-state studies with these catalytic materials. The H_2CO and $(H_3CO)_2CH_2$ mass spectrometer signals were corrected for the minor contributions from the cracking of CH_3OH in the mass spectrometer.

Recent studies by Vohs et al. demonstrated that the same T_p, maximum peak temperature, values can be obtained from model single crystal and powdered supported metal oxide catalytic systems because a significant portion of the intermediate reaction products (e.g., H_2CO) are able to leave the powdered bed without becoming trapped on the catalyst surface and further oxidized to CO_2.[11,12] Furthermore, these very significant studies also demonstrated that the Redhead equation,[1,11,12] typically employed to obtain kinetic parameters from single-crystal temperature-programmed studies in ultrahigh vacuum (UHV), can also be applied to obtain quantitative kinetic parameters from the powdered samples during the CH_3OH-TPSR studies

$$E_a/(RT_p^2) = \upsilon/B \exp(-E_a/(RT_p)) \quad (1)$$

where R is the gas-phase constant, B is the heating rate employed in the temperature programmed study, E_a is the activation energy for the surface reaction, and υ is the first-order Arrhenius rate constant pre-exponential factor. Many previous CH_3OH-TPSR studies with single crystals have shown that formation of H_2-CO from CH_3OH proceeds via a first-order reaction kinetics and a υ that is typically very close to $\sim 10^{13}$ s^{-1}. Consequently, this value for υ was selected to determine the activation energy, E_a, for the first-order surface reactions of methanol from the Redhead equation (eq 1).

Steady-State Methanol Oxidation. The steady-state methanol oxidation studies were conducted in an isothermal fixed-bed reactor operating under differential reaction conditions (methanol conversions less than 10%). The reactor consists of a 3.8 mm glass tube, and the catalyst powder, ~25−100 mg, was held in place by glass wool (above and below the catalyst). The catalysts were pretreated in flowing O_2 at 300 °C prior to the methanol oxidation for the bulk, pure, and supported metal oxide catalysts described above. The bulk mixed metal oxide catalysts were not examined for methanol oxidation since preliminary studies demonstrated that TeO_x was volatile under the oxidizing reaction conditions employed for methanol oxidation (methanol/O_2/He mixture of 6/13/81). Analysis of the reaction products was performed with an online gas chromatograph (HP-5840A) containing two packed columns (Porapak R and Carbosieve SII) and two detectors (thermal conductivity detector and flame ionization detector). The steady-state reaction temperature was maintained at 230 °C.

The steady-state methanol oxidation catalytic data were expressed in terms of turnover frequency, TOF, by normalizing the reaction rate per surface metal oxide site. For the supported metal oxides, the reaction rate was normalized per number of active surface sites of the supported component, which assumed 100% dispersion and was independently confirmed with Raman spectroscopy. For the bulk metal oxides, the number of active surface sites was determined by methanol chemisorption and that value was multiplied by a factor of 3 to account for the known ratio of $CH_3OH/M \sim 3$ due to lateral interactions in the chemisorbed methanol monolayer.[5−8,11,12] The ratio of CH_3-$OH/M \sim 3$ was obtained with model supported metal oxide systems containing monolayer surface coverage, and it was assumed that the same stoichiometry also holds for bulk metal oxides. The steady-state methanol oxidation kinetic expression at low conversions and over an oxidized metal oxide surface has been shown to be[13]

$$TOF = k_{rds}K_{ads}(P_{CH_3OH})^1(P_{O_2})^0 \ (s^{-1}) \quad (2)$$

where k_{rds} is the first-order Arrhenius rate constant for the rate-determining-step, K_{ads} is the methanol equilibrium adsorption constant, and P_{CH_3OH} is the methanol partial pressure in the gas phase. The reaction is zero-order in oxygen partial pressure in the gas phase because the catalyst surfaces are fully oxidized under reaction conditions.[9] The value for the first-order surface rate constant, k_{rds}, is independently obtained from the CH_3OH-TPSR experiments. This independent kinetic information allows for direct determination of K_{ads} from the steady-state methanol oxidation TOF value, eq 2, as shown below

$$K_{ads} = TOF(P_{CH_3OH})^1/k_{rds} \ (L/mol) \quad (3)$$

Furthermore, the methanol equilibrium heat of adsorption on the catalyst, ΔH_{ads}, can also be determined from the following relationship

$$\Delta H_{ads} = E_{app} - E_a \ (kcal/mol) \quad (4)$$

where E_a is the activation energy for the first-order surface reaction obtained from the CH_3OH-TPSR experiments (see eq 1 above) and E_{app} is the apparent activation energy for steady-state methanol oxidation.[14] Previous studies over many metal oxide catalysts revealed that the E_{app} for methanol oxidation to formaldehyde was typically ~20 kcal/mol,[13,14] and consequently, this value for E_{app} was employed to determine the methanol equilibrium heat of adsorption on the metal oxide surface.

Results

CH_3OH-TPSR Studies with Model Supported Metal Oxide Catalysts. Before the studies with the bulk Mo−V−Nb−Te−O mixed metal oxide catalytic materials were initiated, CH_3OH-TPSR studies with model supported metal oxide catalysts were undertaken because these model systems contain the supported active metal oxide components as a two-dimensional metal oxide monolayer (100% dispersion) and their surface compositions can be controlled. The model supported metal oxide catalysts investigated consisted of molybdena, vanadia, telluria, and their combinations supported on Nb_2O_5. Niobia was selected as the support since it is the only oxide present in the mixed Mo−V−Nb−Te−O metal oxide system that possesses high surface areas after calcinations at 450 °C. Raman characterization of the model niobia supported metal oxides demonstrated that the 6% MoO_3/Nb_2O_5, 7% V_2O_5/Nb_2O_5, 5% TeO_2/Nb_2O_5, 1% V_2O_5/6% MoO_3/Nb_2O_5, and 1% TeO_2/6% MoO_3/Nb_2O_5 catalysts did not possess crystalline phases and contained monolayer surface coverage of these two-dimensional surface metal oxide species.[15]

The CH_3OH-TPSR spectrum for the Nb_2O_5 support is presented in Figure 1. The formation of dimethyl ether (DME,

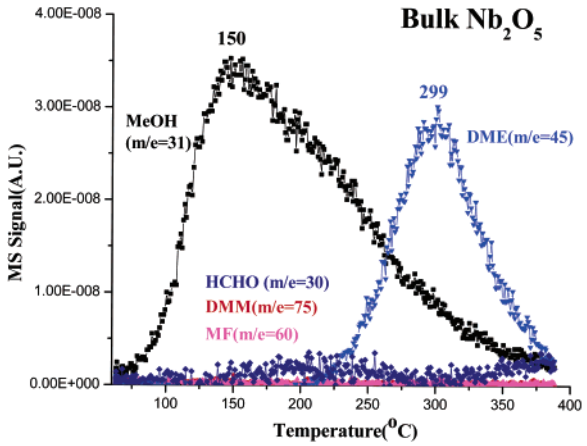

Figure 1. CH_3OH-TPSR from bulk Nb_2O_5.

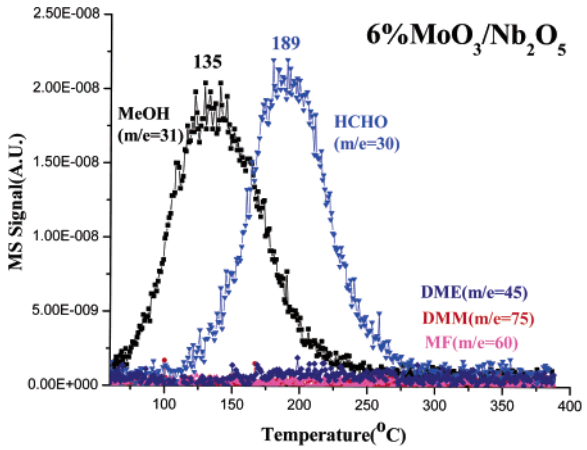

Figure 2. CH_3OH-TPSR from supported 6% MoO_3/Nb_2O_5.

CH_3OCH_3) with a $T_p \sim 300$ °C originates from surface methoxy reactions over surface acidic sites. These are weak acidic sites since pyridine adsorption IR measurements did not detect any surface acidic sites on the calcined Nb_2O_5.[16] Desorption of CH_3OH with a $T_p \sim 150$ °C is primarily due to molecularly adsorbed methanol and is also obtained when the adsorption temperature is further decreased toward room temperature. The high-temperature tail of the CH_3OH curve originates from surface methoxy (*OCH_3) species that become rehydrogenated by surface hydroxyls to form CH_3OH during the TPSR experiment. No formation of H_2CO from surface redox sites is observed.[17] Thus, the Nb_2O_5 support contains weak surface Lewis acid sites that convert the surface methoxy (*OCH_3) species to DME and also back to CH_3OH. The elementary steps of the DME formation reaction are not known in the literature, but isotopic experiments with deuterated methanol suggest that the rate-determining-step (rds) does not involve breaking of C−H or O−H bonds and, thus, involves first-order scission of the C−O bond of the surface methoxy intermediate.[17]

The CH_3OH-TPSR spectra for the model supported 6% MoO_3/Nb_2O_5 catalyst are presented in Figure 2. The chemisorbed surface methoxy species yields H_2CO with a T_p of ∼189 °C and CH_3OH with a T_p of ∼135 °C over surface redox sites. Deuterium isotopic labeling studies demonstrated that the first-order rds involves breaking of the methyl C−H bond of the surface methoxy intermediate to form H_2CO and CH_3OH.[17] The reaction products of DME, DMM, and MF are not observed during this CH_3OH-TPSR experiment. As the CH_3OH-TPSR cycles are repeated without reoxidizing the surface MoOx species (not shown for brevity), the H_2CO formation peak

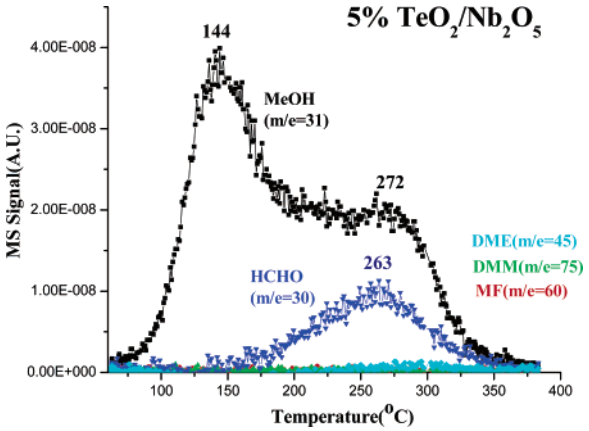

Figure 3. CH_3OH-TPSR from supported 5% TeO_2/Nb_2O_5.

temperature shifts from 189 °C toward ∼211 °C as the surface Mo^{6+} sites become reduced to lower oxidation states (formation of formaldehyde is accompanied by extraction of one oxygen atom from the surface MoO_x species to make H_2O). The shift in T_p to higher temperatures is reflected in an order of magnitude decrease in the Arrhenius k_{rds} rate constant. In addition, the amount of H_2CO formed continuously decreases and the amount of CH_3OH formation continuously increases. The continuous decrease in the formation of H_2CO with repeated CH_3OH-TPSR cycles reveals that reduced surface MoO_x species do not dissociatively chemisorb methanol as efficiently as the fully oxidized surface Mo^{6+} redox sites. Furthermore, no DME is formed at ∼300 °C, which indicates that all the surface Nb acidic sites of the Nb_2O_5 support have been titrated by the surface molybdena species.

The CH_3OH-TPSR experiments for the model supported 7% V_2O_5/Nb_2O_5 catalyst give the same spectra as that for the corresponding model supported 6% MoO_3/Nb_2O_5 catalyst, with the exception of slightly different T_p values and ratio of H_2CO/CH_3OH. The formation of H_2CO on the redox surface vanadia sites occurs at ∼177 °C rather than ∼189 °C over the redox surface molybdena sites, reflecting the higher activity of the surface vanadia sites than the surface molybdena sites on Nb_2O_5. Another difference between surface vanadia and molybdena species is the much higher production of H_2CO and lower production of CH_3OH from the 7% V_2O_5/Nb_2O_5 catalyst. These observations suggest that the methanol equilibrium adsorption constant, K_{ads}, is probably higher for surface vanadia than surface molybdena species. The H_2CO TPSR peaks also shift to higher temperatures as the surface vanadia sites are reduced by repeated cycles of CH_3OH-TPSR, but its reduction is more sluggish. Vohs et al. nicely demonstrated by combining CH_3OH-TPSR and XPS analysis, on single crystals of TiO_2 and CeO_2 containing a surface vanadia monolayer, that H_2CO formation occurs with a T_p ∼100 °C lower from surface V^{5+} sites than on surface V^{3+} sites.[11,12] This translates to at least 2 orders of magnitude in activity between the k_{rds} values of surface V^{5+} and V^{3+} sites. The absence of DME formation reveals that the surface vanadia species cover the surface acidic sites of the Nb_2O_5 support.

The CH_3OH-TPSR spectrum for the model supported 5% TeO_2/Nb_2O_5 catalyst is shown in Figure 3. The selective oxidation reaction products from this oxidized surface are H_2CO ($T_p \sim 263$ °C) and CH_3OH ($T_p \sim 144$ and ∼272 °C). The simultaneous formation of H_2CO and CH_3OH at 263−272 °C reflects the redox nature of the surface TeO_x species on the Nb_2O_5 support.[17] Desorption of CH_3OH with $T_p \sim 144$ °C originates from molecularly adsorbed methanol. The absence

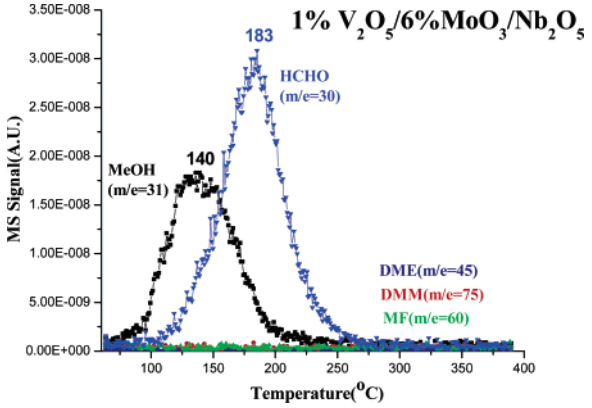

Figure 4. CH_3OH-TPSR from supported 1% V_2O_5/6% MoO_3/Nb_2O_5.

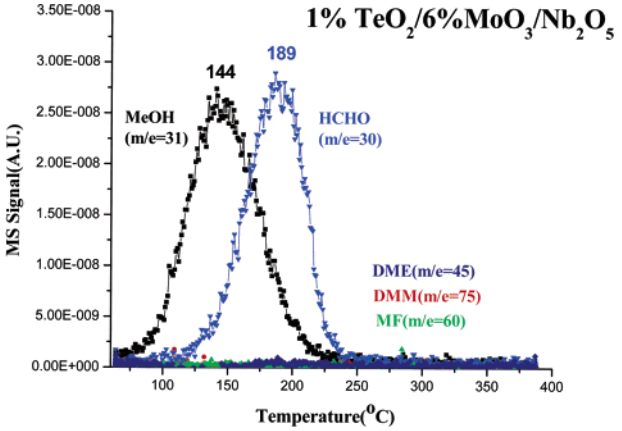

Figure 5. CH_3OH-TPSR from supported 1% TeO_2/6% MoO_3/Nb_2O_5.

of DME formation demonstrates that the surface acidic sites on the Nb_2O_5 support are also titrated by the surface telluria species. The surface telluria species possess redox characteristics that exhibit a significantly lower activity relative to the other surface redox sites ($V^{5+} > Mo^{6+} \gg Te^{4+}$).

The above CH_3OH-TPSR studies demonstrate that the individual oxides among Mo, V, Te, and Nb give rise to different reaction products, ratios of product to methanol, and specific T_p values and that the T_p values are also dependent on the specific oxidation states. These experiments, however, do not provide any information about what happens when multiple metal oxides are simultaneously present on the surface. To address this issue, studies with supported mixed metal oxide monolayer catalysts were also undertaken. The CH_3OH-TPSR spectrum from the model supported 1% V_2O_5/6% MoO_3/Nb_2O_5 catalyst is shown in Figure 4. Interestingly, the H_2CO production at $T_p \sim 183$ °C is somewhat lower than that originally observed for 6% MoO_3/Nb_2O_5 due to the addition of 1% V_2O_5 to the surface molybdena monolayer on niobia. This reveals that the surface chemistry of this mixed metal oxide monolayer is being dominated by the surface V^{5+} species and that the surface methoxy species are able to surface diffuse toward the surface V^{5+} sites during the TPSR experiment. The rapid surface diffusion of $Mo-OCH_3$ and $V-OCH_3$ was demonstrated in previous studies.[18] Furthermore, the same T_p value for 5% V_2O_5/Nb_2O_5 and 1% V_2O_5/6% MoO_3/Nb_2O_5 also reveals that the kinetics for methoxy decomposition of the surface vanadia species on Nb_2O_5 are not influenced by the presence of surface molybdena species. The increase in reactivity is also reflected in the much higher production of H_2CO/CH_3OH in the presence of surface vanadia. To examine the kinetic behavior of the introduction of a cation with lower activity, the model supported 1% TeO_2/6% MoO_3/Nb_2O_5 catalyst system was also investigated with CH_3OH-TPSR. The resultant CH_3OH-TPSR spectrum shown in Figure 5 is almost indistinguishable from the previous results for the surface Mo^{6+} sites on the Nb_2O_5 support (reflected in the same T_p values and ratio of H_2CO/CH_3OH). These findings again reflect the surface mobility of the surface methoxy intermediates and their preferred reaction pathway to H_2CO formation via the most active surface sites ($V^{5+} > Mo^{6+} \gg Te^{4+}$).

The CH_3OH-TPSR results above for the Nb_2O_5 supported metal oxide catalysts are collected in Table 1 for comparison: T_p, k_{rds}, K_{ads}, E_a, and H_2CO/CH_3OH, DME/CH_3OH, or CO_2/CH_3OH ratios.

CH_3OH-TPSR Studies with Bulk, Pure Metal Oxides. The CH_3OH-TPSR spectrum for bulk Nb_2O_5 was already presented in Figure 1 and revealed that only surface acidic sites are present on this metal oxide and form DME from the surface methoxy species. From pyridine-IR chemisorption studies, however, it was found that the calcined Nb_2O_5 did not possess surface Lewis or Bronsted acid sites as probed by pyridine.[16] It appears that methanol is able to sense some weak surface acidic sites on the Nb_2O_5 since it exclusively forms DME on this metal oxide surface.

The CH_3OH-TPSR spectra from bulk V_2O_5 are depicted in Figure 6 as a function of several TPSR cycles without exposure to gas-phase oxygen between each cycle. The formation of H_2CO from the surface methoxy species always occurs with a $T_p \sim 188$ °C, and the peak temperature does not change position with each subsequent reducing cycle. The relatively constant T_p of ~188 °C suggests that primarily active surface V^{5+} redox sites are present on the bulk V_2O_5 powders. The ability to maintain the surface V^{5+} sites fully oxidized implies that oxygen anions are diffusing from the bulk lattice to the surface to reoxidize the surface V cations reduced by the CH_3OH-TPSR experiment (Mars−van Krevelen mechanism). The decrease in the H_2CO formation is due to some sintering of this thermally fragile material during the TPSR experiment. The decrease in the H_2CO/CH_3OH ratio with each CH_3OH-TPSR cycle reveals that some surface reduced VO_x sites are also present and that these reduced sites do not chemisorb methanol as readily as the more active surface V^{5+} redox sites. No DME formation was observed reflecting the absence of active surface acidic sites for this sample under the current experimental conditions.[17]

The CH_3OH-TPSR spectra from bulk MoO_3 are shown in Figure 7 as a function of CH_3OH-TPSR cycles. Unlike bulk V_2O_5 reduction cycles, the H_2CO T_p for MoO_3 initially occurs at ~196 °C and continuously increases toward 221 °C with each reduction cycle. This change is analogous to the reduction of surface V^{5+} to V^{4+}/V^{3+} observed by Vohs et al.[11,12] and reflects the reduction of the surface Mo species with each cycle. The ease of reduction of the surface Mo^{6+} sites to lower oxidation states with each cycle reflects the inability of bulk lattice oxygen of MoO_3 to diffuse to the surface and fully reoxidize the reduced Mo cations under the current experimental conditions. The reduction in the amount of H_2CO formed with each cycle is due to sintering of this thermally fragile metal oxide and the creation of surface reduced MoO_x sites that decrease methanol chemisorption on the defective MoO_3 surface. The decrease in the H_2CO/CH_3OH ratio with each cycle reflects the lower methanol K_{ads} on the partially reduced molybdena surface. The significant shifts in T_p translate to about an order of magnitude decrease in k_{rds} for the conversion of surface methoxy to H_2CO on MoO_3. The lack of DME formation reveals the absence of surface acidic sites on the surface of MoO_3 for the present catalyst and experimental conditions.

TABLE 1: Quantitative Determination of Parameters from CH_3OH-TPSR and Steady-State Methanol Oxidation Experiments.

catalyst	TOF (s^{-1}) $\times 10^{-3}$ at 230 °C	T_p (°C) of HCHO	T_p (°C) of DME	rel HCHO production with the adsorption cycle	HCHO/CH_3OH	DME/CH_3OH	k_{rds} (s^{-1}) @ 230 °C for HCHO− not Nb_2O_5	K_{ads} (L/mol)	E_a (kcal/mol)
6% MoO_3/Nb_2O_5 (1st)	18	189	*	100.0	1.02	*	0.20	0.6×10^2	31.5
6% MoO_3/Nb_2O_5 (2nd)		195	*	92.3	0.84	*	0.13	*	31.9
6% MoO_3/Nb_2O_5 (3rd)		210	*	63.3	0.69	*	0.05	*	33.0
6% MoO_3/Nb_2O_5 (4th)		211	*	50.1	0.57	*	0.04	*	33.1
7% V_2O_5/Nb_2O_5	85	177	*	*	*	*	0.47	1.2×10^2	30.7
5% TeO_2/Nb_2O_5		263	*	*	0.20	*	1.1×10^{-3}	*	36.7
1% V_2O_5/6% MoO_3/Nb_2O_5		183	*	*	1.39	*	0.31	*	31.1
1% TeO_2/6% MoO_3/Nb_2O_5		189	*	*	0.89	*	0.20	*	31.5
V_2O_5 (first)	87	188	*	100.0	3.73	*	0.22	273.7	31.5
V_2O_5 (second)		188	*	91.5	1.45	*	0.22	*	31.5
V_2O_5 (third)		188	*	69.2	1.58	*	0.22	*	31.5
MoO_3 (first)	18	196	*	100.0	1.26	*	0.12	99.3	32.0
MoO_3 (second)		213	*	74.6	1.00	*	0.04	*	33.2
MoO_3 (third)		221	*	69.3	0.91	*	0.02	*	33.8
TeO_2	0.6	432	*	*	0.10	*	0.72×10^{-8}	0.6×10^8	48.7
Nb_2O_5	7	*	299	*	0.00	0.493	8×10^{-5}	5.4×10^4	39.3
$Mo_{0.6}V_{1.5}O_x$		173	*	*	0.45	*	0.62	*	30.4
$Mo_{1.0}V_{0.5}Te_{0.16}O_x$		175	*	*	0.82	*	0.54	*	30.5
$Mo_{1.0}V_{0.3}Te_{0.16}Nb_{0.12}O_x$		173	146	*	0.39	0.24	0.62	*	30.4

[a] The TOF and K_{ads} values were obtained from steady-state methanol oxidation studies and the remaining parameters were obtained from CH_3OH-TPSR studies.

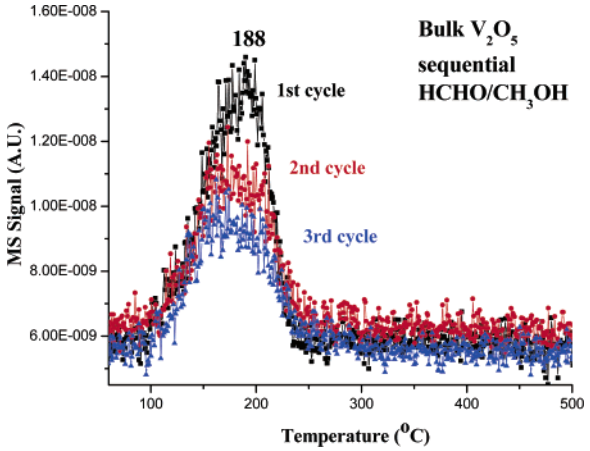

Figure 6. CH_3OH-TPSR from bulk V_2O_5, several cycles.

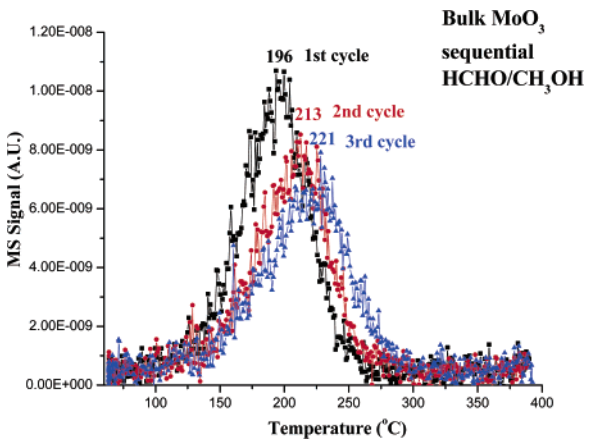

Figure 7. CH_3OH-TPSR from bulk MoO_3, several cycles

Unlike the fully oxidized bulk and model supported V_2O_5 and MoO_3 catalysts that gave similar T_p temperatures for H_2-CO formation, the T_p values for bulk TeO_2 and supported 5% TeO_2/Nb_2O_5 varied by ~170 °C. This dramatic decrease in T_p temperatures for the formation of these reaction products reveals that the niobia support is promoting the catalytic activity of the surface telluria species. Such a dramatic decreases in the T_p corresponds to an increase in k_{rds} of more than 5 orders of magnitude. A closer examination of the bulk and supported vanadia and molybdena catalysts also shows that the T_p values appear to slightly decrease when these metal oxides are deposited on the Nb_2O_5 support (e.g., V^{5+} decreases from ~188 to 177 °C and Mo^{6+} decreases from 196 to 189 °C). The absence of surface acidic sites is reflected in the CH_3OH-TPSR product yield containing no DME.

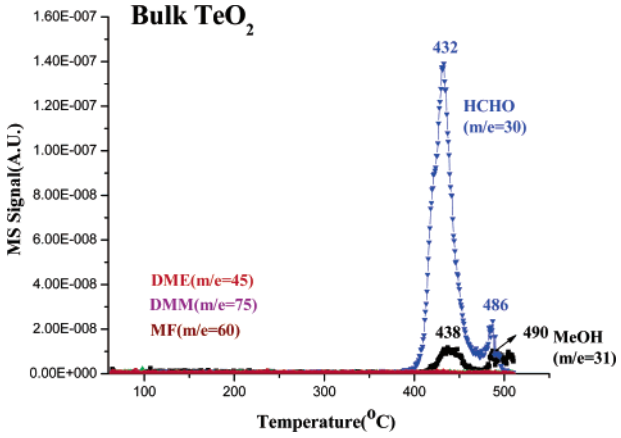

Figure 8. CH_3OH-TPSR from bulk TeO_2.

The CH_3OH-TPSR results for the bulk, pure Nb_2O_5, V_2O_5, MoO_3, and TeO_2 metal oxides are presented in Table 1 for comparison: T_p, k_{rds}, K_{ads}, E_a, and H_2CO/CH_3OH or DME/CH_3-OH ratios.

CH_3OH-TPSR Studies with Bulk Mixed Metal Oxides. Prior to undertaking the CH_3OH-TPSR experiments, the Raman spectra of the mixed metal oxides were examined for phase purity and structural changes. The Raman spectra of the bulk mixed metal oxides are compared against the reference MoO_3 and V_2O_5 crystalline Raman spectra in Figure 9. Comparison of the Raman spectra of bulk MoO_3 and V_2O_5 with that of bulk $M_{0.6}V_{1.5}O_x$ reveals that the binary mixed metal oxide phase is monophasic, does not contain separate small V_2O_5 or MoO_3 crystallites, and has a structure uniquely different from its two

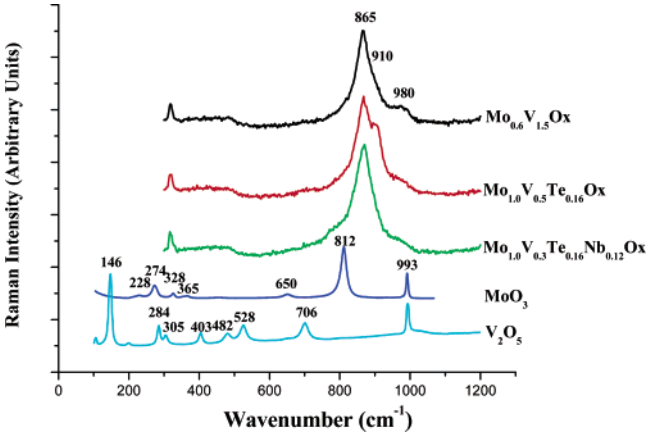

Figure 9. Raman spectra of bulk $Mo_{0.6}V_{1.5}O_x$, $Mo_{1.0}V_{0.5}Te_{0.16}O_x$, $Mo_{1.0}V_{0.3}Te_{0.16}Nb_{0.12}O_x$, MoO_3, and V_2O_5 metal oxides.

pure metal oxide components. The Raman spectrum of bulk $Mo_{0.6}V_{1.5}O_x$ appears to be similar to a distorted MoO_3 structure since it exhibits a strong band at ~865 cm^{-1}, rather than 812 cm^{-1}, and a much weaker band at ~980 cm^{-1}, rather than 993 cm^{-1}. The bulk $Mo_{0.6}V_{1.5}O_x$ Raman spectrum is dominated by the bulk vibrations of molybdena rather than vanadia because of the much higher Raman scattering cross section of molybdenum oxides than vanadium oxides. By analogy with the well-known vibrations of crystalline MoO_3, the band at ~865 cm^{-1} is assigned to Mo−O−Mo and Mo−O−V vibrations and the band at ~980 is assigned to Mo═O and/or V═O vibrations. The decrease in the relative intensity of the ~980 cm^{-1} band with increasing Mo/V ratio suggests that this band probably arises mostly from V═O vibrations. As the Mo content of the mixed oxides is increased in the tertiary and quaternary mixed oxides, Mo/V ratio from 0.4 to 3.3, the corresponding Raman spectra do not change very much relative to that of the binary $Mo_{0.6}V_{1.5}O_x$ because of the higher molybdenum oxide contents, the much stronger Raman scattering cross section of the Mo−O vibrations (Mo > V−O > Nb−O > Te−O), and the similar bulk Mo oxide structures.

The influence of different reactive environments upon the bulk structure of the quaternary $Mo_{1.0}V_{0.3}Te_{0.16}Nb_{0.12}O_x$ was also examined with in situ Raman spectroscopy, but the spectra are not shown for brevity. The quaternary mixed oxide bulk structure was found to be stable to dehydration in He at 350 °C, exposure to CH_3OH/He at 250 °C, and various C_3H_8/O_2 reaction environments (C_3H_8/O_2 ratios from 6/1 to 1/1). A very small crystalline MoO_3 Raman band was only found to be present under propane ODH conditions. However, this corresponds to only a trace of crystalline MoO_3 because of the very strong Raman scattering cross section of this band. Thus, the mixed metal oxide bulk structure appears to be relatively stable under reactive environments that are not net oxidizing.

The surface of the binary bulk $Mo_{0.6}V_{1.5}O_x$ mixed metal oxide was found to only yield H_2CO product from surface methoxy species on surface redox sites at T_p ~ 173 °C (see Figure 10), which corresponds to the surface V^{5+} sites (see Table 1). The shift of the H_2CO T_p value from ~188 to ~173 °C from the pure V_2O_5 to the bulk $Mo_{0.6}V_{1.5}O_x$ mixed metal oxide, respectively, reflects the promotion of V^{5+} sites by adjacent cation ligands. The surface of the tertiary bulk $Mo_{1.0}V_{0.5}Te_{0.16}O_x$ mixed metal oxide system was found to only yield H_2CO at T_p ~ 175 °C, which is also characteristic of surface V^{5+} redox sites promoted by adjacent cation ligands (see Figure 11). The surface of the quaternary bulk $Mo_{1.0}V_{0.3}Te_{0.16}Nb_{0.12}O_x$ mixed metal oxide was found to yield both DME (T_p ~ 146 °C) and H_2CO

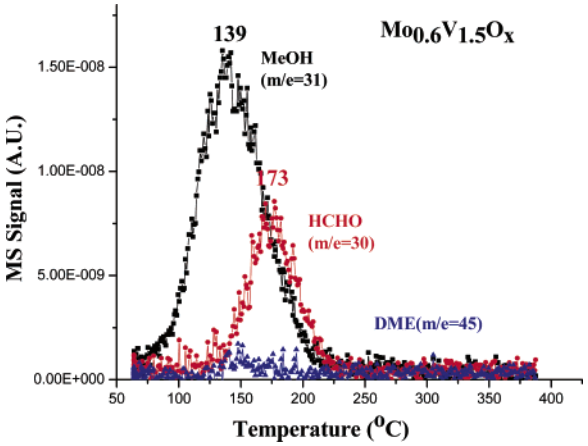

Figure 10. CH_3OH-TPSR from bulk $Mo_{0.6}V_{1.5}O_x$.

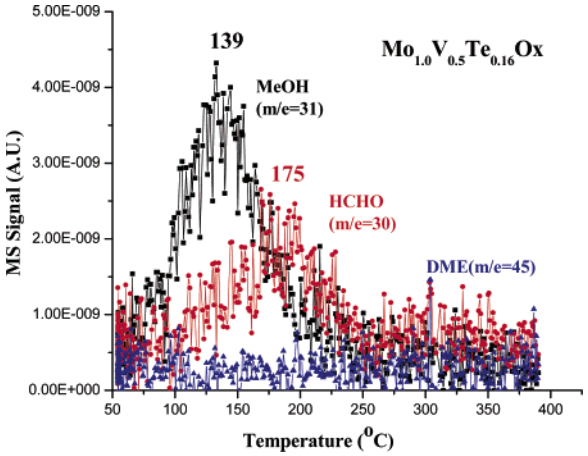

Figure 11. CH_3OH-TPSR from bulk $Mo_{1.0}V_{0.5}Te_{0.16}O_x$.

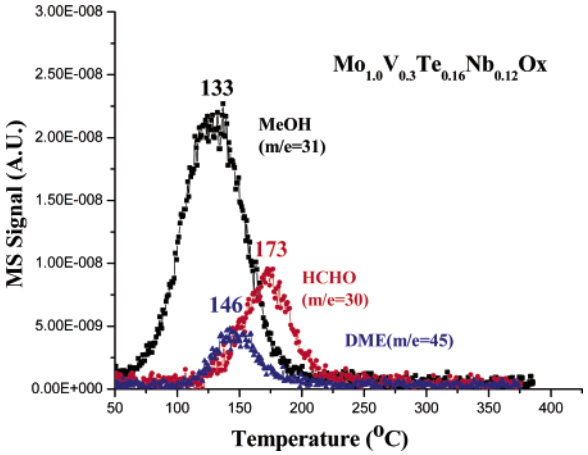

Figure 12. CH_3OH-TPSR from bulk $Mo_{1.0}V_{0.3}Te_{0.16}Nb_{0.12}O_x$.

(T_p ~ 173 °C), as shown in Figure 12. The surface redox sites for H_2CO formation at T_p ~ 173 °C also correspond to surface V^{5+} sites promoted by the other cations that were already found for the binary and tertiary bulk mixed metal oxide catalysts. The surface acidic sites for DME formation at T_p ~ 146 °C correspond to surface Mo^{6+} sites promoted by the other cations. Although the supported 6% MoO_3/Nb_2O_5 catalyst and bulk MoO_3 did not give rise to DME formation in this low-temperature region, other supported molybdena catalysts (e.g., MoO_3/Al_2O_3, MoO_3/TiO_2, and MoO_3/ZrO_2) did exhibit the formation of DME at the same temperatures.[19] The formation of DME in this temperature range was not observed for other supported metal oxide catalysts (e.g., V_2O_5, CrO_3, Re_2O_7, WO_3,

Ta_2O_5, etc.).[19] Thus, the surface V^{5+} sites are responsible for redox chemical properties of all three mixed metal oxides and only the quaternary mixed oxide system also exhibits the acidic chemical property typically associated with surface Mo^{6+} sites.

The CH_3OH-TPSR results for the bulk mixed metal oxides are presented in Table 1 for comparison: T_p, k_{rds}, K_{ads}, E_a, and H_2CO/CH_3OH or DME/CH_3OH ratios.

Discussion

Surface Elemental Composition of Bulk Mixed Metal Oxide Catalysts. The CH_3OH-TPSR spectra demonstrated that each of the fully oxidized surface Mo, V, Te, and Nb oxides possesses a different reactivity temperature window: V ($T_p \sim$ 173−188 °C), Mo ($T_p \sim$ 189−196 °C), Te (∼260−430 °C), and Nb (∼300 °C). Thus, it is possible to use this surface chemistry knowledge to discriminate among the different surface metal oxide species present for the mixed metal oxide catalysts. The CH_3OH-TPSR spectra, however, may sometimes also be dominated by the most active surface sites due to the high surface mobility of the surface $*OCH_3$ species[18] and, consequently, may not provide as much information about less reactive surface catalytic sites. This appears to be the case for the less reactive surface Te^{4+} and Nb^{5+} oxides that are overshadowed by the more active surface V^{5+} and Mo^{6+} sites. Thus, to obtain a complete elemental analysis of the outermost surface layer of mixed metal oxides, it is also necessary to perform surface physical characterization with the surface sensitive low-energy ion-scattering spectroscopy (LEISS)[20] to complement the CH_3OH-TPSR chemical characterization. In addition, the surface sensitive LEISS characterization investigations will also determine if various reactive environmental treatments (e.g., H_2, CH_3OH, C_3H_8, C_3H_8/O_2, etc.) can alter the surface composition of mixed metal oxides.

The surface enrichment in V^{5+} for bulk $Mo_{0.6}V_{1.5}O_x$ is not too surprising because of the high vanadia content (71 atomic %) of this bulk mixed oxide. The surface enrichment in V^{5+} for bulk $Mo_{1.0}V_{0.5}Te0_{0.16}O_x$ and $Mo_{1.0}V_{0.3}Te_{0.17}Nb_{0.12}O_x$, however, is somewhat surprising since the bulk V atomic contents of these mixed oxides are only 30% and 19%, respectively. The enriched surface V^{5+} sites on the mixed metal oxide surfaces is related to the high mobility of the V^{5+} cation and the driving force to decrease to surface free energy of the mixed metal oxide system. The enhanced mobility of V^{5+} is associated with its much lower Tammann temperature, defined as half the melting point, of V_2O_5 (209 °C) compared to the other metal oxides TeO_2 (230 °C), MoO_3 (261 °C), and Nb_2O_5 (620 °C). The Tammann temperature represents the temperature that surface atoms of a material begin to diffuse and suggests that the mobility of V^{5+} is greater than that the other metal cations. The surface free energy of surfaces terminating with M═O bonds (e.g., V_2O_5 and MoO_3) is significantly less than surfaces terminating with M−OH bonds (e.g., TeO_2 and Nb_2O_5).[18] Thus, the much higher mobility of V^{5+} relative to the other metal cations coupled with its ability to minimize the surface free energy of mixed metal oxide systems is apparently responsible for its surface enrichment of these bulk mixed metal oxides.

Surface Oxidation States of Bulk Mixed Metal Oxide Catalysts. For those active surface cations that dominate the CH_3OH-TPSR spectra, the T_p position also reflects the cation oxidation state. Vohs et al. nicely demonstrated that for supported vanadia monolayer catalysts the T_p value for the surface vanadia species varies ∼100 °C depending on the vanadia cation oxidation state.[10−12] A similar trend also occurs for reduced surface molybdena species (see Table 1). The cyclic CH_3OH-TPSR experiments with the molybdena catalysts also revealed that this method is also sensitive to the simultaneous presence of fully oxidized and partially reduced surface metal oxide cations. Furthermore, by performing several reducing cycles of CH_3OH-TPSR it is possible to determine if the surface cations are being reoxidized by *bulk* or *surface* lattice oxygen via a Mars−van Krevelen reaction mechanism. CH_3OH-TPSR cyclic studies over bulk V_2O_5 revealed that methanol oxidation during TPSR proceeds by a *bulk* Mars−van Krevelen mechanism involving bulk lattice oxygen since the same T_p value was obtained. In contrast, the CH_3OH-TPSR studies over bulk MoO_3 demonstrated that methanol oxidation during TPSR proceeds with the participation of primarily *surface* lattice oxygen since the T_p value increased with each reduction cycle. These findings reveal that O^{2-} diffusion through the bulk V_2O_5 lattice is much faster than O^{2-} diffusion through the bulk MoO_3 lattice. The current CH_3OH-TPSR experiments suggest that the surfaces of the bulk mixed metal oxide catalysts investigated in the present study consist of fully oxidized surface V and Mo sites after calcination in N_2.

Surface Chemical Nature of Bulk Mixed Metal Oxide Catalysts. For metal oxides, it is critical to know the chemical nature of the surface metal oxide cations, which cannot be provided by physical characterization methods. Fortunately, methanol oxidation over metal oxides produces different reaction products depending on the surface chemistry of the specific metal oxide: H_2CO from surface redox sites, DME from surface acidic sites, and CO_2 from surface basic sites. The latter assumes that CO_2 is the primary product and does not originate from overoxidation of H_2CO or from surface deposition of carbonaceous molecules from the background.[17] Surface redox sites are able to readily give up their bridging oxygen in M−O−S bonds and surface acidic sites are not capable of giving up their bridging oxygen in bridging M−O−S bonds and possess either Bronsted acidity, H^+, or Lewis acidity, oxygen vacancies that are electron deficient.[16] Surface basic sites are electron rich and readily accept molecules containing H^+ or that are electron poor. Steady-state methanol oxidation over the pure MoO_3, V_2O_5, TeO_2, and Nb_2O_5 demonstrated that only redox and acidic reaction products are obtained for low methanol conversions.[21] From this information it is possible to conclude from CH_3OH-TPSR results that surface vanadia, molybdena, and telluria sites are redox and surface niobia sites are acidic in nature. Although higher alcohols, such as 2-propanol, can also determine the nature of active surface sites, they are much more sensitive to the acidic surface sites because of their more facile unimolecular dehydration reactions compared to the more demanding bimolecular CH_3OH dehydration reaction to form DME.[21]

Surface Reactivity of Bulk Mixed Metal Oxide Catalysts. The first-order Arrhenius rate constants for the rate-determining-steps, k_{rds}, of the various methanol oxidation surface reactions are quantified from the T_p values obtained from the CH_3OH-TPSR spectra and are presented in Table 1. It is clear that surface V^{5+} is about an order of magnitude more active than surface Mo^{6+}, which in turn is ∼100 times more active than Te^{4+}, for methanol oxidation to H_2CO. The surface Nb^{5+} sites are not very active for methanol dehydration to DME and reflect the presence of weak surface Lewis acid sites.[16] The significant effect reduction has on the surface cation oxidation state is also apparent from the k_{rds} values. For example, surface $V^{5+} > V^{4+} \gg V^{3+}$ and the k_{rds} spans a factor of ∼100 in going from V^{5+} to V^{3+}.[11,12] Furthermore, the effect of promoting ligands on the catalytic activity is directly quantifiable by the changes in the T_p values. For example, H_2CO formation from surface V^{5+}

present on bulk V_2O_5 exhibits a $T_p \sim 188$ °C and from surface V^{5+} promoted by neighboring Mo^{6+} in the bulk mixed oxides exhibits a $T_p \sim 173$ °C, which translates to a kinetic factor of ~3 in the first-order k_{rds} value. This promotion is most probably related to the lower Sanderson electronegativity of adjacent Mo^{6+} (2.2) and Nb^{5+} (1.42) cations relative to the V^{5+} (2.51) and Te^{4+} (2.62) cations.[22] The lower electronegativity of adjacent cations would increase the partial negative charge on the bridging V−O−M bonds (where M is either Mo or Nb). This would further increase the basic character of the bridging oxygen atom and enhance its affinity for accepting H atoms from the adsorbing methanol molecule and the surface methoxy intermediate. It also accounts for the activity enhancement observed when the surface Mo^{6+}, V^{5+}, and Te^{4+} are supported on Nb_2O_5, which possesses the lowest electronegativity among these four.

Adsorption Equilibrium Constants of Bulk Mixed Metal Oxides. Combination of the k_{rds} values obtained from the CH_3OH-TPSR studies and the corresponding steady-state reaction rates, TOF, allows for the direct determination of the K_{ads} values. This calculation assumes that the surface metal oxide sites are fully oxidized and, thus, cannot be applied to the partially reduced metal oxide surfaces. The methanol adsorption equilibrium constants, K_{ads}, are shown in Table 1 for those oxide catalysts that have been examined for steady-state methanol oxidation. From the current limited available data in Table 1, it is not clear if any relationships exist between K_{ads} and the k_{rds} values for methanol oxidation. However, such a relationship was found to hold for supported vanadia catalysts with different oxide supports since both the dissociative CH_3OH chemisorption and surface CH_3O^* decomposition to H_2CO involve transfer of an H atom to basic oxygen.

Lattice Oxygen Transport in Bulk Metal Oxides. Cyclic CH_3OH-TPSR studies revealed the interesting observation that the surface of bulk V_2O_5 was readily reoxidized by bulk lattice oxygen after being reduced by CH_3OH, but that the surface of MoO_3 was not rapidly reoxidized by the bulk lattice oxygen and remained reduced after methanol reduction. This result is unexpected since previous studies of bulk lattice oxygen diffusion in V_2O_5 and MoO_3 indicated that the oxygen mobilities in these metal oxides were essentially identical.[23,24] The origin of this difference in oxygen diffusion measurements may be that the current studies are only probing the *outermost layer* and a limited number of layers below the surface, the surface region, rather than solid-state diffusion of bulk lattice oxygen in bulk metal oxides. These interesting findings suggest that for catalytic applications the bulk lattice oxygen mobility in the surface region may be different than the more typical bulk lattice oxygen transport usually measured for bulk metal oxides.

Oxidative Dehydrogenation of Propane to Propylene. To examine the applicability of the CH_3OH-TPSR findings to other oxidation reactions, the bulk and supported Mo−V−Te−Nb−O mixed metal oxide catalysts were compared to earlier reactivity data for propane oxidative dehydrogenation to propylene.[15] For propane ODH, the reactivity order of the fully oxidized bulk and niobia supported catalysts followed the pattern $V^{5+} > Mo^{6+} \gg Te^{4+}$. The propane ODH findings exactly parallel the CH_3OH-TPSR reactivity pattern above that the surface $V^{5+} > Mo^{6+} \gg Te^{4+}$ for methanol oxidative dehydrogenation to H_2CO. This parallel trend between propane and methanol ODH is consistent in that the rate-determining steps in both oxidative dehydrogenation reactions being the breaking of a C−H bond. In situ Raman studies reveal that the surface metal oxide species present in the supported metal oxide catalysts are essentially fully oxidized under reaction conditions employing excess gas-phase oxygen.[24] This observation is in agreement with the conclusion that for supported vanadia catalysts the surface lattice oxygen from the surface vanadia species is involved in propane ODH from oxygen isotopic labeling experiments and the zero-order dependence on the oxygen partial pressure.[25] This catalytic reactivity pattern also seems to be applicable for propylene selective oxidation to acrolein studies over supported vanadia catalysts currently in progress.[26] It has been shown that propane selective oxidation to acrylic acid over the bulk Mo−V−Te−Nb−O mixed metal oxide catalysts exhibits a zero-order dependence on the oxygen partial pressure and first-order dependence on the propane partial pressure,[27] which implies a Mars−van Krevelen reaction mechanism using *surface* or *bulk* lattice oxygen from the catalyst in the rate-determining-step. The current bulk V_2O_5 and MoO_3 CH_3OH-TPSR cyclic reduction studies revealed that it would also be possible to discriminate between *surface* and *bulk* Mars−van Krevelen reaction mechanisms for this bulk mixed metal oxide catalyst. Thus, it seems that the CH_3OH-TPSR spectroscopy findings in the current investigation are not only limited to methanol oxidation studies but also can be generalized to other hydrocarbon oxidation reactions.

Conclusions

The CH_3OH-TPSR experiments have shown to be able to provide fundamental surface information about the nature of the active surface sites present on the *outermost surface layer* of bulk Mo−V−Te−Nb−O mixed metal oxides. The T_p values are sensitive to each specific cation and reflect surface compositional information. Furthermore, the T_p values are also sensitive to the presence of reduced surface cations since the T_p values shift to higher values from partially reduced surface cations. This latter characteristic can also be applied to determine if a Mars−van Krevelen reaction mechanism over bulk mixed oxides proceeds via a *bulk* or *surface* lattice oxygen. The chemical nature of the active surface sites is reflected in the methanol oxidation reaction products formed (e.g., H_2CO from surface redox sites and DME from surface acidic sites). Determination of the T_p values allows for the direct quantification of the corresponding Arrhenius rate constant k_{rds}, the surface reaction constant for the rate-determining step of the decomposition of the surface methoxy intermediate to formaldehyde. Changes in the T_p or k_{rds} values reflect the promotion of the active redox sites by neighboring cation ligands that influence the electron density on the bridging oxygen in M−O−S bonds. Knowledge of the corresponding steady-state TOF value also allows the determination of K_{ads}, the equilibrium adsorption constant. The combination of CH_3OH-TPSR and LEISS studies is ideally suited to advance our fundamental knowledge about the chemical nature of the *outermost layer* of bulk mixed metal oxide catalysts in the coming years. Molecular structural information about the active surface sites present in the *outermost layer* of mixed metal oxides still awaits the development of novel physical spectroscopic surface characterization methods and the use of model mixed metal oxide systems.[28]

Application of this approach to characterizing the surface of the bulk Mo−V−Te−Nb−O mixed metal oxides revealed that the active surface sites consisted of surface V^{5+} and Mo^{6+} cations and that the role of Nb^{5+} and Te^{4+} cations may primarily be as promoter ligands. The most active and selective bulk mixed metal oxide catalyst, the quaternary Mo−V−Te−Nb−O system, was found to possess both surface V^{5+} redox and surface Mo^{6+} acidic sites. Comparison of the current CH_3OH-TPSR

findings with corresponding propane ODH catalytic studies suggests that the findings from CH_3OH-TPSR are also be applicable to other hydrocarbon oxidation reactions. Thus, this new CH_3OH-TPSR spectroscopy approach to obtaining surface information about bulk mixed metal oxide catalysts is providing much new and needed rich chemical insights about the surface properties of bulk mixed metal oxide catalysts that previously were not attainable by other characterization methods.

Acknowledgment. This research work was sponsored by the Department of Energy-Basic Energy Sciences (Grant DEFG02-93ER14350). Israel E. Wachs wishes to dedicate this paper to Michel Boudart for introducing him to the kinetics of heterogeneous catalytic reactions in the course on "Kinetics of Chemical Processes" in the winter of 1974, and for his mentoring during his graduate school days as well as after graduation from Stanford University. Michel Boudart has had a profound influence on Wachs' scientific career in heterogeneous catalysis for the past 30 years.

References and Notes

(1) Boudart, M.; Djega-Mariadassou, G. *Kinetics of Heterogeneous Catalysis*; Princeton University Press: Princeton, NJ, 1984.

(2) Emmettt, P. H.; Brunauer, S. *J. Am. Chem. Soc.* **1937**, *59*, 310, 1553.

(3) Djega-Mariadassou, G.; Marques, A. R.; Davignon, L. *J. Chem. Soc., Faraday Trans. 1* **1982**, *78*, 2447.

(4) Farneth, W.; Staley, R. H.; Sleight, A. W. *J. Am. Chem. Soc.* **1986**, *108*, 2327. Farneth, W. E.; Ohuchi, F.; Staley, R.; Chowdry, U.; Sleight, A. W. *J. Phys. Chem.* **1985**, *89*, 2493.

(5) Briand, L. E.; Farneth, W.; Wachs, I. E. *Catal. Today* **2000**, *62*, 219.

(6) Briand, L. E.; Hirt, A. M.; Wachs, I. E. *J. Catal.* **2001**, *202*, 268.

(7) Briand, L. E.; Jehng, J. M.; Cornaglia, L. M.; Hirt, A. M.; Wachs, I. E. *Catal. Today* **2003**, *78*, 257.

(8) Burcham, L. J.; Briand, L. E.; Wachs, I. E. *Langmuir* **2001**, *17*, 6164;. Burcham, L. J.; Briand, L. E.; Wachs, I. E. *Langmuir* **2001**, *17*, 6175.

(9) Burcham, L. J.; Deo, G.; Gao, X.; Wachs, I. E. *Top. Catal.* 2000, *11/12*, 85.

(10) Zhang, Z.; Henrich, V. E. *Surf. Sci.* **1992**, *277*, 263. Guo, Q.; Lee, S.; Goodman, D. W. *Surf. Sci.* **1999**, *437*, 38. Sambi, M.; Sangiovanni, G.; Granozzi, G.; Parmiagiani, F. *Phys. Rev. B* **1997**, *55*, 7850. Wong, G. S.; Kragten, D. D.; Vohs, J. M. *Surf. Sci.* **2000**, *452*, L293. Wang, Q.; Madix, R. J. *Surf. Sci.* **2001**, *474*, L213.

(11) Wong, G. S.; Concepcion, M. R.; Vohs, J. M. *Surf. Sci.* **2003**, 211.

(12) Feng, T.; Vohs, J. M. *J. Catal.* **2002**, *208*, 301.

(13) Holstein, W. L.; Machiels, C. J. *J. Catal.* **1996**, *162*, 118.

(14) Deo, G.; Wachs, I. E. *J. Catal.* **1994**, *146*, 323, 335.

(15) Zhao, Z.; Wachs, I. E. *J. Phys. Chem. B* **2003**, *107*, 6333.

(16) Datka, J.; Turek, A. M.; Jehng, J.-M.; Wachs, I. E. *J. Catal.* **1992**, *135*, 186. Jehng, J.-M.; Turek, A. M.; Wachs, I. E. *Appl. Catal., A* **1992**, *83*, 179.

(17) Tatibouet, J. M. *Appl. Catal., A* **1997**, *148*, 213. Tatibouet, J. M.; Lauron-Pernot, H. *J. Mol. Catal. A: Chem.* **2001**, *171*, 2005.

(18) Wang, C. B.; Cai, Y.; Wachs, I. *Langmuir* **1999**, *15*, 1223.

(19) Kim, T.; Wachs, I. E. To be submitted for publication.

(20) Briand, L. E.; Tkachenko, O. P.; Guraya, M.; Wachs, I. E.; Gruenert, W. *Surf. Interface Anal.* **2004**, *36*, 238. Briand, L. E.; Tkachenko, O. P.; Guraya, M.; Gao, X.; Wachs, I. E. *J. Phys. Chem. B* **2004**, *108*, 4823.

(21) Badlani, M.; Wachs, I. *Catal. Lett.* **2001**, *75*, 137. Kulkarni, D.; Wachs, I. E. *Appl. Catal., A* **2002**, *237*, 121.

(22) Sanderson, R. T. *J. Chem. Educ.* **1988**, *65*, 112.

(23) Boreskov, G. In *Catalysis Science and Technology*; Anderson, J. R., Boudart, M., Eds.; Springer: New York, Vol. 3, p 62.

(24) Kapoor, R.; Oyama, S. T. *J. Mater. Res.* **1997**, *12*, 467.

(25) Gao, X.; Jehng, J.-M.; Wachs, I. E. *J. Catal.* **2002**, *209*, 43.

(26) Chen, K.; Khodakov, A.; Yang, J.; Bell, A. T.; Iglesia, E. *J. Catal.* **2000**, *186*, 325. Chen, K.; Xie, S.; Iglesia, E.; Bell, A. T. *J. Catal.* **2000**, *192*, 197. Chen, K.; Bell, A. T.; Iglesia, E. *J. Phys. Chem. B* **2000**, *104*, 1292.

(27) Zhao, C.; Wachs, I. E. To be submitted for publication.

(28) Katou, T.; Vitrry, D.; Ueda, W. *Chem. Lett.* **2003**, *32*, 1028.

(29) Schlogl, R. The Impact of In Situ Analysis of Heterogeneous Catalysts for the Improvement of Their Function. Presentation at the Meeting of the Catalysis and Chemical Transformations Programs; Office of Basic Energy Sciences, Department of Energy, U.S.: Rockville, MD, May 23−26, 2004.